第 35 卷第 1 期 无 机 化 学 学 报 Vol.35 No.1
2019 年 1 月 CHINESE JOURNAL OF INORGANIC CHEMISTRY 133-140

以 4,4′-(1-咪唑基亚甲基)二苯甲酸为配体的锌配合物的合成、晶体结构和荧光性质

喻 敏 宣 芳 刘光祥*
(南京晓庄学院环境科学学院,新型功能材料南京市重点实验室,南京 211171)

摘要:以 $Zn(NO_3)_2·6H_2O$ 和 4,4′-(1-咪唑基亚甲基)二苯甲酸(H_2IMB)为原料,在不同溶剂热条件下反应,得到 2 个结构不同的配合物$[Zn(HIMB)_2]_n$ (**1**)和$\{[Zn(IMB)]·1.5H_2O\}_n$ (**2**),对它们进行了 X 射线单晶衍射分析、元素分析、红外光谱分析、热重分析和粉末衍射。配合物 **1** 属于正交晶系,$C222_1$ 空间群,a=0.935 2(3) nm,b=2.583 3(8) nm,c=1.396 4(4) nm,V=3.373 6(18) nm^3,Z=4,M_r=707.98,D_c=1.394 g·cm^{-3},μ=0.786,F(000)=1 456,R_1=0.048 6,wR_2=0.120 1(I>2σ(I))。配合物 **2** 属于四方晶系,$I4_1/acd$ 空间群,a=1.853 5(2) nm,b=1.853 5(2) nm,c=4.309 7(5) nm,V=14.806 (4) nm^3,Z=32,M_r=412.69,D_c=1.481 g·cm^{-3},μ=1.360,F(000)=6 752,R_1=0.043 7,wR_2=0.117 1(I>2σ(I))。单晶结构分析显示,配合物 **1** 拥有二维二重贯穿聚索烃格子状层状结构,而配合物 **2** 具有三维二重贯穿(3,6)-连接$(6^{11}.8^4)(6^3)_2$ 网状结构。结果说明了溶剂在配合物组装过程中起着非常重要的作用。此外,还研究了 2 个配合物的荧光性质。

关键词:锌配合物;双官能团配体;晶体结构;荧光性质
中图分类号:O614.24+2 **文献标识码**:A **文章编号**:1001-4861(2019)01-0133-08
DOI:10.11862/CJIC.2019.018

Syntheses, Crystal Structures and Photoluminescent Properties of Two Zinc(Ⅱ) Coordination Polymers Derived from 4,4′-((1*H*-Imidazol-1-yl)methylene)dibenzoic Acid

YU Min XUAN Fang LIU Guang-Xiang*
(*Nanjing Key Laboratory of Advanced Functional Materials, School of Environmental Science, Nanjing Xiaozhuang University, Nanjing* 211171, *China*)

Abstract: Two zinc(Ⅱ) coordination polymers, $[Zn(HIMB)_2]_n$ (**1**) and $\{[Zn(IMB)]·1.5H_2O\}_n$ (**2**), (H_2IMB=4,4′-((1*H*-imidazol-1-yl)methylene)dibenzoic acid), have been synthesized and characterized by IR spectroscopy, elemental analyses, thermogravimetric analysis (TGA), powder X-ray diffraction (PXRD), and single-crystal X-ray diffraction. Complex **1** crystallizes in orthorhombic, space group $C222_1$ with a=0.935 2(3) nm, b=2.583 3(8) nm, c=1.396 4(4) nm, V=3.373 6(18) nm^3, M_r=707.98, D_c=1.394 g·cm^{-3}, F(000)=1 456, μ=0.786 mm^{-1} and Z=4. The final R_1=0.048 6 and wR_2=0.120 1 for 2 794 observed reflections when I>2σ(I). Complex **2** belongs to tetragonal, space group $I4_1/acd$ with a=1.853 5(2) nm, b=1.853 5(2) nm, c=4.309 7(5) nm, V=14.806 (4) nm^3, M_r=412.69, D_c=1.481 g·cm^{-3}, F(000)=6 752, μ=0.136 0 mm^{-1} and Z=32. The final R_1=0.043 7 and wR_2=0.117 1 for 3 615 observed reflections when I>2σ(I). Structural analyses reveal that complex **1** shows a 2D→2D polycatenane of 2-fold interpenetrated sql layer, whereas complex **2** possesses a 3D 2-fold interpenetrated (3,6)-connected net with the point symbol of $(6^{11}.8^4)(6^3)_2$. The results show that the solvent plays a significant role in the structure of the final products. CCDC: 1851301, **1**; 1851302, **2**.

Keywords: zinc(Ⅱ) coordination polymer; bifunctional ligand; crystal structure; luminescence

收稿日期:2018-07-30。收修改稿日期:2018-10-30。
国家自然科学基金(No.21671107)资助项目。
*通信联系人。E-mail:njuliugx@126.com

The design and synthesis of coordination polymers (CPs) have continued unabated over the past decade. These materials possess diverse and enticing applications in gas storage and separation, sensing, ion exchange, heterogeneous catalysis, non-linear optics, explosives residue detection, luminescence and even drug delivery[1-8]. However, the applications of CPs are directly related to their structural features. Thus, the fabrication of desired CPs with the targeted structures and properties has become a great challenge for research scientists owing to many key factors including metal ions, organic ligands, metal-ligand ratio, pH, reaction solvents, temperature, as well as the oxidation state of the metal ion[9-12]. Among them, the design and judicious selection of organic ligands are of crucial concern in the CP construction because the structure, symmetry, solubility, size, and coordination mode of these ligands directly correlate with the architectures of CPs[13-16]. Generally speaking, multifunctional ligands are the first choice for the construction of coordination polymers because they are sensitive to pH value of the reaction solution and can adopt variety of coordination modes to bridge metal ions[17-20]. Here, the 4,4′-((1*H*-imidazol-1-yl) methylene)dibenzoic acid (H_2IMB) ligand was chosen as the linker, and the reasons are as follows: flexible carboxyphenyl and rigid imidazolyl group can provide multidentate metal-binding sites and diverse coordination modes; the varying coordination modes of the ligands have great potential in synthesizing different coordination polymers with intriguing structures and unique properties[21-23]. Moreover, it is equally important that the metal ions have a d^{10} configuration to construct coordination polymers with an excellent luminescent property[24-26]. Motivated by these abovementioned aspects, we obtain two new coordination polymers, namely, $[Zn(HIMB)_2]_n$ (**1**) and $\{[Zn(IMB)]\cdot 1.5H_2O\}_n$ (**2**). Herein, we report their syntheses, crystal structures and luminescent properties.

1 Experimental

1.1 Materials and general methods

All reagents and solvents employed in this work were commercially available and used without further purification. The H_2IMB ligand was purchased from WuXi AppTec Group. Elemental analyses (C, H and N) were performed on a Vario EL Ⅲ elemental analyzer. Infrared spectra were recorded on KBr discs using a Nicolet Avatar 360 spectrophotometer in the range of 4 000 ~400 cm^{-1}. The luminescent spectra for the powdered solid samples were measured at ambient temperature on a Horiba FluoroMax-4P-TCSPC fluorescence spectrophotometer. Powder X-ray diffraction (PXRD) measurements were performed on a Bruker D8 Advance diffractometer at 40 kV, 40 mA with Cu $K\alpha$ radiation (λ=0.154 056 nm) and a graphite monochromator scanning from 5° to 50° at room temperature.

1.2 Synthesis of $[Zn(HIMB)_2]_n$ (1)

A mixture containing $Zn(NO_3)_2\cdot 6H_2O$ (29.6 mg, 0.1 mmol) and H_2IMB (32.2 mg, 0.1 mmol) in 15 mL of DMF/CH_3OH/H_2O (1∶2∶2, *V*/*V*) mixed solution was sealed in a 25 mL Teflon lined stainless steel container and heated at 100 ℃ for 3 days. Colorless block crystals of **1** were collected by filtration and washed with water and ethanol several times with a yield of 44% based on H_2IMB ligand. Anal. Calcd. for $C_{36}H_{26}N_4O_8Zn$(%): C, 61.07; H, 3.70; N, 7.91. Found(%): C, 60.98; H, 3.72; N, 7.93. IR (KBr, cm^{-1}): 3 457 (br), 3 139 (w), 1 702 (s), 1 561 (s), 1 521 (s), 1 419 (m), 1 391 (s), 1 273 (w), 1 208 (m), 1 122 (w), 997 (w), 892 (m), 835 (w), 782 (w), 651 (w), 565 (w), 542 (w).

1.3 Synthesis of $\{[Zn(IMB)]\cdot 1.5H_2O\}_n$ (2)

A mixture containing $Zn(NO_3)_2\cdot 6H_2O$ (29.6 mg, 0.1 mmol) and H_2IMB (32.2 mg, 0.1 mmol) in 15 mL of DMF/H_2O (2∶1, *V*/*V*) mixed solution was sealed in a 25 mL Teflon lined stainless steel container and heated at 100 ℃ for 3 days. Colorless pillar crystals of **2** were collected by filtration and washed with water and ethanol several times with a yield of 26% based on H_2IMB ligand. Anal. Calcd. for $C_{18}H_{15}N_2O_{5.5}Zn$ (%): C, 52.38; H, 3.66; N, 6.79. Found (%): C, 52.47; H, 3.65; N, 6.81. IR (KBr, cm^{-1}): 3 473 (br), 3 165 (w), 1 608 (s), 1 519 (m), 1 422 (s), 1 377 (s), 1 273 (m), 1 123 (w), 1 034 (w), 1 010 (s), 871 (m), 835 (w), 778 (w), 659 (m), 527 (m).

1.4 X-ray crystallography

Two single crystals with dimensions of 0.22 mm×0.16 mm×0.08 mm for **1** and 0.18 mm×0.14 mm×0.10 mm for **2** were mounted on glass fibers for measurement, respectively. X-ray diffraction intensity data were collected on a Bruker APEX Ⅱ CCD diffractometer equipped with a graphite-monochromatic Mo $K\alpha$ radiation (λ=0.071 073 nm) using the φ-ω scan mode at 293(2) K. Data reduction and empirical absorption correction were performed using the SAINT and SADABS program[27], respectively. The structures were solved by the direct method using SHELXS-2016[28] and refined by full-matrix least squares on F^2 using SHELXL-2016[29]. All of the non-hydrogen atoms were refined anisotropically. The solvent molecules in **2** were highly disordered and were removed from the diffraction data by the SQUEEZE routine of PLATON program. The final formula of **2** were determined by single-crystal structures, elemental analysis results and TGA. The details of the crystal parameters, data collection and refinement for **1** and **2** are summarized in Table 1, and selected bond lengths and angles with their estimated standard deviations are listed in Table 2.

CCDC: 1851301, **1**; 1851302, **2**.

Table 1　Crystal data and structure refinement for 1 and 2

Complex	**1**	**2**
Formula	$C_{36}H_{26}N_4O_8Zn$	$C_{18}H_{15}N_2O_{5.5}Zn$
Formula weight	707.98	412.71
Temperature	293(2)	293(2)
Crystal system	Orthorhombic	Tetragonal
Space group	$C222_1$	$I4_1/acd$
a / nm	0.935 2(3)	1.853 5(2)
b / nm	2.583 3(8)	1.853 5(2)
c / nm	1.396 4(4)	4.309 7(5)
V / nm^3	3.373 6(18)	14.806 (4)
Z	4	32
D_c / (g·cm^{-3})	1.394	1.481
Absorption coefficient / mm^{-1}	0.786	1.360
θ range / (°)	2.92~25.50	2.84~27.50
F(000)	1 456	6 752
Reflection collected	23 866	200 087
Independent reflection	3 153 (R_{int}=0.067 1)	4 248 (R_{int}=0.061 5)
Reflection observed [$I>2\sigma(I)$]	2 794	3 615
Data, restraint, parameter	3 153, 0, 223	4 248, 0, 226
Goodness-of-fit on F^2	1.016	1.098
R_1, wR_2 [$I>2\sigma(I)$]	0.048 6, 0.120 1	0.043 7, 0.117 1
R_1, wR_2 (all data)	0.059 5, 0.127 6	0.052 5, 0.124 6
Largest difference peak and hole / (e·nm^{-3})	472 and −257	470 and −349

Table 2　Selected bond lengths (nm) and angles (°) for 1 and 2

1					
Zn(1)-O(2)	0.197 7(4)	Zn(1)-N(1)#2	0.202 7(5)		
O(2)-Zn(1)-O(2)#1	98.7(3)	O(2)#1-Zn(1)-N(1)#2	104.29(19)	O(2)#1-Zn(1)-N(1)#3	113.81(19)
O(2)-Zn(1)-N(1)#2	113.81(19)	O(2)-Zn(1)-N(1)#3	104.29(19)	N(1)#2-Zn(1)-N(1)#3	120.1(3)

Continued Table 2

2					
Zn(1)-N(1)#1	0.202 2(3)	Zn(1)-O(3)#2	0.198 6(2)	Zn(1)-O(4)#3	0.196 0(2)
Zn(1)-O(1)	0.195 4(3)				
O(1)-Zn(1)-N(1)#1	129.36(13)	O(1)-Zn(1)-O(4)#3	116.64(12)	O(4)#3-Zn(1)-N(1)#1	102.24(12)
O(1)-Zn(1)-O(3)#2	97.13(11)	O(3)#2-Zn(1)-N(1)#1	92.83(11)	O(4)#3-Zn(1)-O(3)#2	116.51(10)

Symmetry codes: #1: $-x$, y, $-z+1/2$; #2: $-x+1$, $-y+1$, $z+1/2$; #3: $x-1$, $-y+1$, $-z$ for **1**; #1: $y-1/4$, $-x+3/4$, $z+1/4$; #2: $y-3/4$, $x+1/4$, $z+1/4$; #3: $-y+3/4$, $-x+5/4$, $z+1/4$ for **2**.

2 Results and discussion

2.1 Crystal structure

Single crystal X-ray diffraction analysis revealed that complex **1** crystallizes in the orthorhombic space group $C222_1$ and features a 2D→2D polycatenane of 2-fold interpenetrated *sql* layer. As illustrated in Fig. 1, the asymmetric unit of complex **1** contains a half zinc ion located on a crystallographic 2-fold axis and one crystallography independent $HIMB^-$ anion. The central Zn(Ⅱ) ion is four-coordinated by two carboxylate oxygen atoms from two $HIMB^-$ anions, and two nitrogen atoms from two other $HIMB^-$ anions in a distorted tetrahedral coordination geometry. Bond lengths and angles about the zinc ion are standard for tetrahedral coordination (Table 2). The central carbon of $HIMB^-$ anion shows sp^3 hybridization, exhibiting C(N)-$N_{central}$-C angles of 111.9(5)°, 111.7(6)° and 114.8(5)°. The dihedral angles between the phenyl rings of the $HIMB^-$ anion are 88.25°, 84.64° and 66.18°, and the $N_{central}$-C(N) bond lengths are 0.148 0(8), 0.153 3(9) and 0.153 2(9) nm, respectively. In **1**, adjacent Zn(Ⅱ) centers are linked by partially deprotonation $HIMB^-$ anions to generate Zn-HIMB chains, which are further extended by $HIMB^-$ anions to form a puckered sheet with Zn⋯Zn distance of 1.171 6 nm (Fig.2). The sheet has only a kind of rhombic window of $Zn_4(HIMB)_4$ with dimensions of 1.870 4 nm×1.396 4 nm.

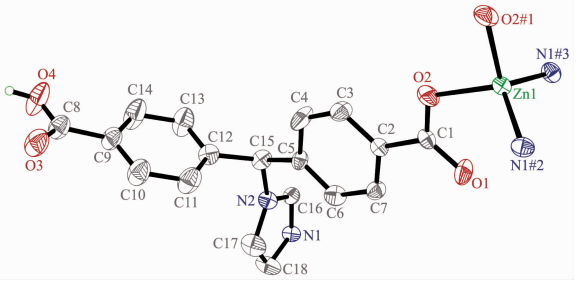

Hydrogen atoms were omitted for clarity; Symmetry codes: #1: $-x$, y, $-z+1/2$; #2: $-x+1$, $-y+1$, $z+1/2$; #3: $x-1$, $-y+1$, $-z$

Fig.1 Coordination environment of the Zn(Ⅱ) ions in **1** with the ellipsoids drawn at the 30% probability level

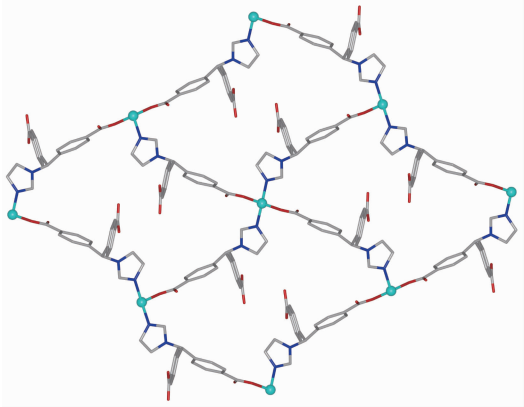

Fig.2 Perspective view of the *sql* layer in **1**

Based on the concept of topology, the layer can be simplified into a (4,4)-connected *sql* net. The potential voids are filled via mutual interpenetration of two independent equivalent networks in a normal mode, giving rise to a 2D→2D polycatenane framework of 2-fold interpenetration (Fig.3). Their mean planes are parallel and coincident. In addition, intramolecular

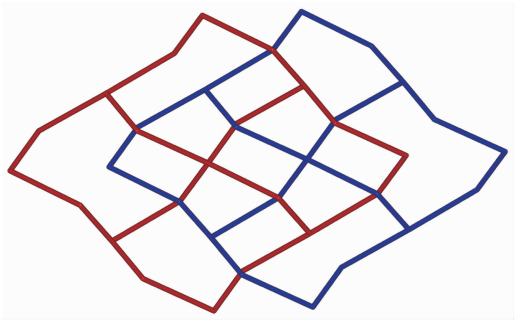

Fig.3 Schematic view of the 2D→2D polycatenane of 2-fold interpenetrated layers

O4–H4…O1 (O4…O1 0.264 1(5) nm) hydrogen-bonding interactions between the layers further stabilize the 2D structure of **1**.

Changing the solution from DMF/CH_3OH/H_2O to DMF/H_2O for the same reaction mixture of **1** affords complex **2**, which crystallizes in the tetragonal $I4_1/acd$ space group and possesses a 3D framework with a dinuclear structure. The asymmetric unit of **2** contains one crystallographically independent Zn(Ⅱ) ion, one individual IMB^{2-} anion as well as one and a half free water molecule. As depicted in Fig.4, each Zn(Ⅱ) ion is four-coordinated by three oxygen atoms from three different IMB^{2-} anions and one nitrogen atom from the imidazole group of IMB^{2-} anions, exhibiting a slightly distorted tetrahedral geometry. All chemical bonds fall in the normal ranges[30].

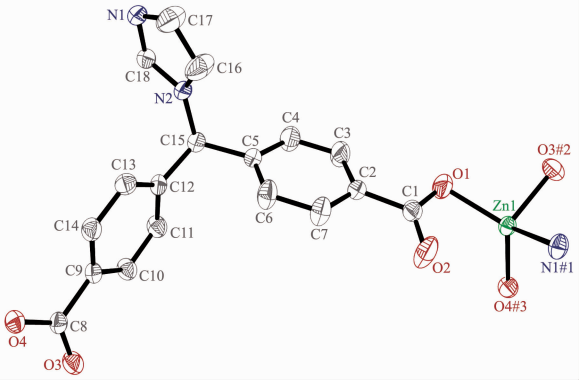

Hydrogen atoms and water molecules were omitted for clarity; Symmetry codes: #1: $y-1/4$, $-x+3/4$, $z+1/4$; #2: $y-3/4$, $x+1/4$, $z+1/4$; #3: $-y+3/4$, $-x+5/4$, $z+1/4$

Fig.4　Coordination environment of the Zn(Ⅱ) ions in **2** with the ellipsoids drawn at the 30% probability level

The central carbon of $HIMB^-$ anion of **2** shows sp^3 hybridization, exhibiting C(N)-$N_{central}$-C angles of 111.9(5)°, 111.7(6)° and 114.8(5)°. The dihedral angles between the phenyl rings of the $HIMB^-$ anion are 88.25°, 84.64° and 66.18°, and the $N_{central}$-C (N) bond lengths are 0.148 0(8), 0.153 3(9) and 0.153 2(9) nm, respectively. In **2**, the H_2IMB ligands are fully deprotonated and the carboxyl groups of IMB^{2-} adopt two coordination modes: μ_2-η^2:η^1 (bis-bridging mode) and μ_1-η^1:η^0 (monodentate mode), and connect two Zn(Ⅱ) ions to generate the dinuclear SBUs $[Zn_2(COO)_2]$ with Zn…Zn distance of 0.375 5 nm (Fig.5). Each IMB^{2-} links three SUBs to give a lattice-shaped 2D layer structure along the c-axis (Fig.6), which is further expanded by IMB^{2-} to form a 3D framework.

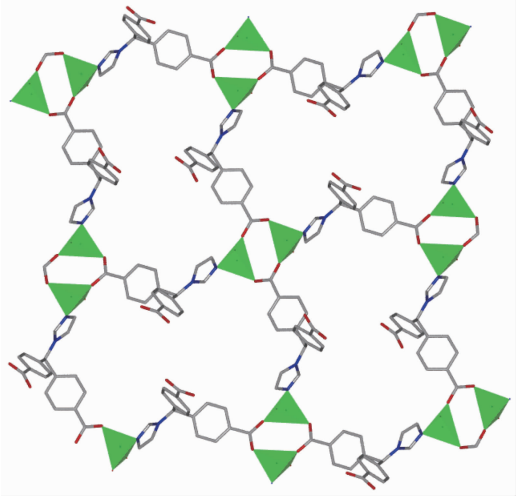

Fig.5　Two dimensional network of **2** viewing along the c-axis

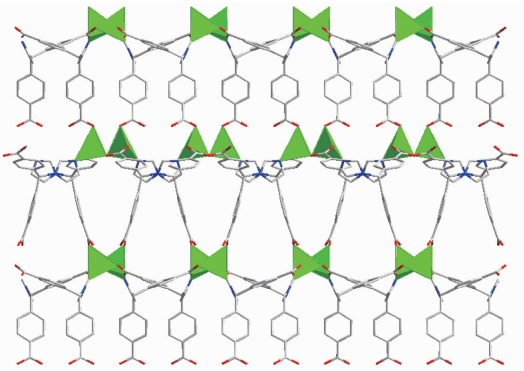

Fig.6　Three dimensional framework of **2** viewing along b direction

By topological analysis, when the dinuclear SBUs are regarded as 6-connected node and the IMB^{2-} as 3-connected node, respectively, the structure of **2** can be simplified as a 2-nodal (3,6)-connected network with the point symbol of $(6^{11}.8^4)(6^3)_2$. Interestingly, two independent equivalent frameworks interlace each other, resulting in a 2-fold interpenetrated 3D framework (Fig.7).

Two different complexes **1** and **2** were synthesized on the basis of the selection of reaction solvent systems, while the other synthetic parameters were intentionally held constant. The dimensionality and topology of the networks produced in this work are

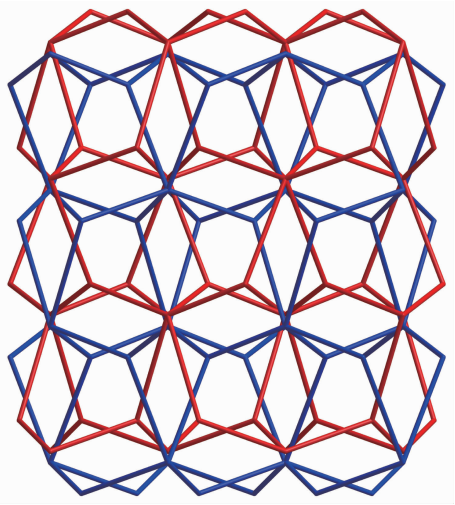

Fig.7 Three dimensional 2-fold interpenetrated (3,6)-connected framework of **2**

determined by the coordination environments of Zn(Ⅱ) ion and linking modes of H_2IMB ligand, which are clearly dictated by the solvent molecules. The solvent not only can affect the extent of deprotonation of organic multicarboxylate ligand but also can induce different conformation of the flexible organic mutilcarboxylate ligand[31-33]. During the self-assemble process, the H_2IMB ligand deprotonated one proton into $HIMB^-$ for **1**, two protons into IMB^{2-} for **2**, respectively. In complex **1**, $HIMB^-$ ligand links two different Zn(Ⅱ) ions in μ_2-N,O coordination mode. While in complex **2**, IMB^{2-} ligand links four different Zn(Ⅱ) ions in μ_2-N, (η^2-O′,O″), (η^1-O′) coordination mode. The different conformations and coordination modes for $HIMB^-$ and IMB^{2-} resulted in structural variation from 2D layer to 3D framework. Thus, the solvent of reaction mixture plays a key role in controlling the structures of the coordination compounds.

2.2 FTIR spectra

The IR spectra of **1** showing the presence of the characteristic bands at 1 702 cm^{-1} indicate the partially deprotonation of H_2IMB, while the IR spectra of **2** showing the absence of the characteristic bands at around 1 700 cm^{-1} attributed to the protonated carboxylate group indicate that the complete deprotonation upon reaction with metal ion. The characteristic bands of carboxyl groups were shown in the range of 1 560~1 610 cm^{-1} for antisymmetric stretching and 1 370~1 420 cm^{-1} for symmetric stretching. The separations ($\Delta\nu$) between $\nu_{asym}(CO_2)$ and $\nu_{sym}(CO_2)$ bands indicate the presence of different coordination modes. The bands in the region 660~1 300 cm^{-1} are attributed to the -CH- in-plane or out-of-plane bend, ring breathing, and ring deformation absorptions of benzene ring, respectively. Weak absorptions observed at 3 139~3 165 cm^{-1} can be attributed to $\nu_{C\text{-}H}$ of benzene ring. The IR spectra exhibited the characteristic peaks of imidazole groups at *ca.* 1 520 cm^{-1} [34].

2.3 Powder X-ray diffraction (PXRD) and thermal analyses

Powder X-ray diffraction analysis (PXRD) experiments were carried out for **1** and *2* at room temperature to characterize their purity. As shown in Fig.8, the measured peak positions closely match the simulated peak positions, indicative of pure products. The thermal behaviors of complexes **1** and **2** were measured under a dry N_2 atmosphere at a heating rate

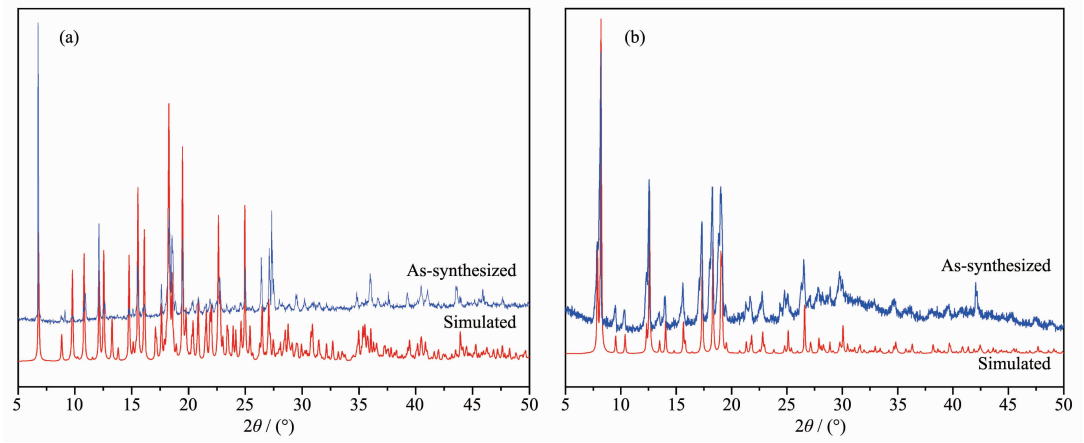

Fig.8 PXRD patterns of complexes **1** (a) and **2** (b)

of 10 ℃·min^{-1} from 25 to 700 ℃ and the TG curves are presented in Fig.9. Complex **1** began to collapse at 210 ℃. Complex **2** lost water molecules before 158 ℃, and the framework began to decompose at 320 ℃.

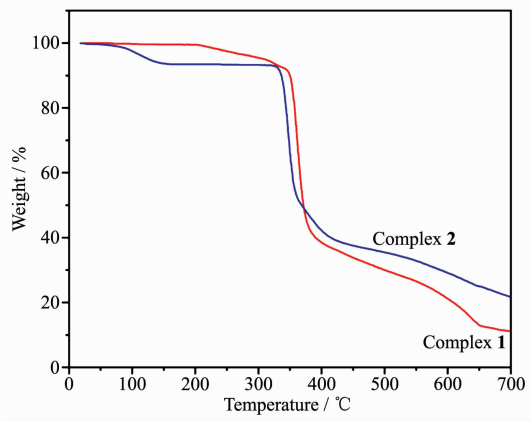

Fig.9　TGA curves of complexes **1** and **2**

2.4　Luminescent properties

Based on the references about the fluorescent properties of Zn complexes[35-38], the solid state luminescent properties of the title complexes and H_2IMB ligand were measured at room temperature under the excitation of 285 nm (Fig.10). The H_2IMB displayed a maximum peak at 462 nm, which is attributed to the $\pi \rightarrow \pi^*$ and $n \rightarrow \pi^*$ transition of intra-ligands. The emission peaks of two complexes occurred at 386 nm (λ_{ex}=315 nm) for **1** and 395 nm (λ_{ex}=323 nm) for **2**, respectively. The emission of **1** and **2** can be essentially ascribed to the intraligand fluorescent emission. The red-shift of the emission can be attributed to the ligand coordination to the metal center, which effectively increases the rigidity of the ligand and reduces the loss of energy by radiationless decay[39-42]. The emission strength of **2** was stronger than complex **1**, which may be caused by different coordination modes.

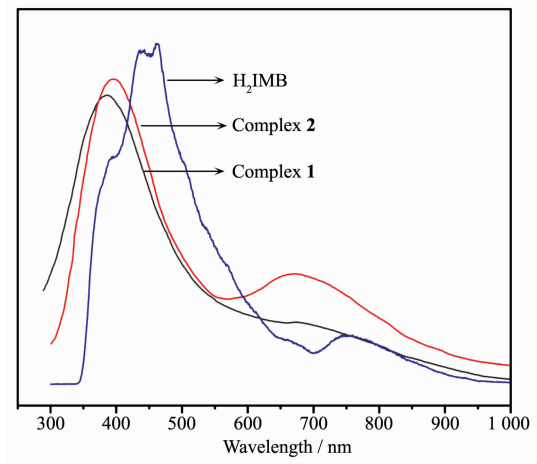

Fig.10　Emission spectra of free H_2IMB ligand, **1** and **2** at room temperature

References:

[1] Lyu H L, Zhang Q, Wang Y, et al. *Dalton Trans.*, **2018**,**47**:4424-4427

[2] Wang H, Lustig W P, Li J. *Chem. Soc. Rev.*, **2018**,**47**:4729-4756

[3] Dutta S, Jana A K, Natarajan S, et al. *Chem. Eur. J.*, **2017**, **23**:8932-8940

[4] Cheng M, Lai C, Liu Y, et al. *Coord. Chem. Rev.*, **2018**,**368**:80-92

[5] Mingabudinaova L R, Vinogradov W, Milichko V A, et al. *Chem. Soc. Rev.*, **2016**,**45**:5408-5431

[6] Wang G Y, Yang L L, Li Y, et al. *Dalton Trans.*, **2013**,**42**:12865-12868

[7] Huang R W, Wei Y S, Dong X Y, et al. *Nat. Chem.*, **2017**,**9**:689-697

[8] Kotzabasaki M, Froudakis G E. *Inorg. Chem. Front.*, **2018**,**5**:1255-1272

[9] Guo X M, Guo H D, Zou H Y, et al. *CrystEngComm*, **2013**,**15**:9112-9120

[10]Zhao F H, Jing S, Che Y X, et al. *CrystEngComm*, **2012**,**14**:4478-4485

[11]Shen L, Gray D, Masel R I, et al. *CrystEngComm*, **2012**,**14**:5145-5147

[12]Guo H D, Guo X M, Zou H Y, et al. *CrystEngComm*, **2014**, **16**:7459-7468

[13]Ding J G, Yin C, Zheng L Y, et al. *RSC Adv.*, **2014**,**4**:24594-24600

[14]Hu F L, Wang S L, Wu B, et al. *CrystEngComm*, **2014**,**16**:6354-6363

[15]Pan M, Su C Y. *CrystEngComm*, **2014**,**16**:7847-7859

[16]LI Tian-Tian(李田田), ZHENG Sheng-Rui(郑盛润). *Chinese J. Inorg. Chem.*(无机化学学报), **2018**,**34**(8):1566-1572

[17]Ye R P, Zhang X, Zhang L, et al. *Cryst. Growth Des.*, **2016**, **16**:4012-4020

[18]Lin Z J, Yang Z, Liu T F, et al. *Inorg. Chem.*, **2012**,**51**:1813-1820

[19]Lin Z J, Huang Y B, Liu T F, et al. *Inorg. Chem.*, **2013**,**52**:3127-3132

[20]Yang J X, Zhang X, Cheng J K, et al. *Cryst. Growth Des.*, **2012**,**12**:333-345

[21]Zhu Z, Xu C G, Wang M, et al. *Cryst. Growth Des.*, **2017**,**17**:

5533-5543

[22]Meng X M, Cui L S, Wang X P, et al. *CrystEngComm*, **2017**, **19**:6630-6643

[23]Yan T, Du L, Sun L, et al. *RSC Adv.*, **2017**,**7**:50150-50155

[24]Wu W P, Liu P, Liang Y T, et al. *J. Solid State Chem.*, **2015**, **228**:124-130

[25]Ma A Q, Wu J, Han Y T, et al. *Dalton Trans.*, **2018**,**47**: 9627-9633

[26]Tian D, Li Y, Chen R Y, et al. *J. Mater. Chem. A*, **2014**,**2**: 1465-1470

[27]Sheldrick G M. *SADABS. Program for Empirical Absorption Correction of Area Detector Data*, University of Göttingen, Germany, **1996**.

[28]Sheldrick G M. *SHELXS*-2016, *Program for Crystal Structure Solution*, University of Göttingen, Germany, **2016**.

[29]Sheldrick G M. *SHELXL*-2016, *Program for the Refinement of Crystal Structure*, University of Göttingen, Germany, **2016**

[30]Wang T, Zhu R R, Zhang X F, et al. *RSC Adv.*, **2018**,**8**: 7428-7437

[31]Song J F, Luo J J, Jia Y Y, et al. *RSC Adv.*, **2017**,**7**:36575-36584

[32]Jing X M, Xiao L W, Wei L, et al. *Inorg. Chem. Commun.*, **2016**,**71**:78-81

[33]Wu Y L, Yang G P, Zhao Y Q, et al. *Dalton Trans.*, **2015**,**44**: 3271-3277

[34]Nakamoto K. *Infrared and Raman Spectra of Inorganic and Coordinated Compounds*. *5th Ed*. New York: Wiley & Sons, **1997**.

[35]Liu Y, Liu W, Xu C, et al. *New J. Chem.*, **2018**,**42**:3885-3891

[36]Arici M, Yesilel O Z, Tas M, et al. *Cryst. Growth Des.*, **2016**, **16**:5448-5459

[37]Li H Q, Ding Z Y, Pan Y, et al. *Inorg. Chem. Front.*, **2016**, **3**:1363-1375

[38]Li H J, He Y L, Li Q Q, et al. *RSC Adv.*, **2017**,**7**:50035-50039

[39]Wen L L, Lu Z D, Lin J G, et al. *Cryst. Growth Des.*, **2007**,**7**: 93-99

[40]Liu H J, Tao X T, Yang J X, et al. *Cryst. Growth Des.*, **2008**,**8**: 259-264

[41]WANG Da-Wei(王大伟), WANG Tao(王滔), YAN Tong(闫桐), et al. *Chinese J. Inorg. Chem.*(无机化学学报), **2017**,**33**(8):1443-1449

[42]de Angelis F, Fantacci S, Sgamellotti A, et al. *Inorg. Chem.*, **2006**,**45**:10576-10584